

# EVALUATION OF THE TIME AND FREQUENCY TRANSFER CAPABILITIES OF A NETWORK OF GNSS RECEIVERS LOCATED IN TIMING LABORATORIES

**Ricardo Píriz**  
GMV Aerospace and Defence, S.A.  
Madrid, Spain  
E-mail: [rpíriz@gmv.com](mailto:rpíriz@gmv.com)

**Giancarlo Cerretto, Andrea Perucca, and Patrizia Tavella**  
Istituto Nazionale di Ricerca Metrologica (INRiM)  
Strada delle Cacce 91, 10135, Torino, Italy  
E-mail: [g.cerretto@inrim.it](mailto:g.cerretto@inrim.it)

## Abstract

*In this paper, we investigate a possible network solution, similar to the IGS Analysis Center solutions, that can be easily managed by a network of timing institutes to solve for all the clock differences (in addition to other quantities) in a unique system to understand the feasibility and the advantages of this approach in time and frequency transfer. The investigation is based on a tool called magicGNSS, which is a Web application for GNSS data processing developed by GMV in Madrid, Spain. magicGNSS allows the users to perform a wide range of calculations and analyses related to GNSS, from the evaluation of performances at user level, to the computation of precise GNSS orbits and clocks, including the calculation of precise receiver coordinates. The time and frequency transfer capabilities of the network solution (named ODTS) are evaluated and compared to PPP solutions as well as to other time transfer results. The possibility to use magicGNSS as an almost near-real-time tool for the comparison of atomic clocks and time scales located in timing laboratories is also addressed.*

## INTRODUCTION

In time metrology, different techniques are used for time and frequency transfer, basically TWSTFT (Two-Way Satellite Time and Frequency Transfer), GPS CV (Common View), and GPS AV (All in View) [1].

In recent years, many national timing laboratories have collocated geodetic GPS receivers together with their traditional GPS/GLONASS CV/AV receivers and TWSTFT equipment. Time and frequency transfer using GPS code and carrier-phase is an important research activity for many institutions involved in time applications, basically due to the fact that carrier-phase measurements generated are two orders of magnitude more precise than the GPS code data. This was recognized when the International GNSS Service (IGS) and the Bureau International des Poids et Mesures (BIPM) formed a joint pilot study to analyze the IGS Analysis Centers clock solutions and recommend new means of combining them. In addition, the CCTF (Consultative Committee for Time and Frequency), in 2006,

passed a recommendation “Concerning the use of Global Navigation Satellite System (GNSS) carrier-phase techniques for time and frequency transfer in International Atomic Time (TAI).” Moreover, the BIPM in 2002 started a project named TAIP3 [2] to examine the use of code and phase measurements.

Many of geodetic GNSS receivers hosted in national timing laboratories operate continuously within the International GNSS Service (IGS) and their data are regularly processed by IGS Analysis Centers. Participating stations must agree to adhere to certain strict standards and conventions that ensure the quality of the IGS Network. A number of products and tools have been developed in order to allow for highly precise time and frequency transfer without taking part in the IGS.

One stand-alone GPS carrier-phase analysis technique is Precise Point Positioning (PPP), in which dual-frequency code and phase measures are used to compare the reference clock of a single receiver to a reference time scale. Several works [3-6] were carried out to evaluate the time and frequency transfer capabilities of PPP, leading the BIPM to start a pilot experiment that aims to evaluate the possibility of regularly computing some TAI links with the PPP algorithm to obtain an improved statistical uncertainty [7]. The PPP algorithm used for the BIPM pilot experiment was developed by the Natural Resources Canada (NRCAN) [8].

## MAGICGNSS

*magicGNSS* is a web application for high-precision GNSS data processing. It allows the calculation of GPS satellite orbits and clocks, and also of station/receiver coordinates, tropospheric delay, and clocks. The user can upload his own station data (RINEX measurement files) and/or use data from a global network of pre-selected *core stations* from IGS.

*magicGNSS* is available at <http://magicgnss.gmv.com>. A free account can be requested online. A \*pro\* account can also be requested with advanced features for professional applications. **In Error! Reference source not found.**, the characteristics of the two *magicGNSS* account types (free and \*pro\*) are reported.

Table 1. Characteristics of *magicGNSS* accounts.

	free	*pro*
Available algorithms	PPP, ODTS, COMP	
Disk quota	1 Gb	10 Gb
Core station data	last 30 days	from 2008/01/01
IGS products <sup>(1)</sup>	last 30 days	from 2000/05/03
Navigation messages <sup>(2)</sup>	last 30 days	from 2008/05/03
User station data in ODTS	no	yes
Max. no. of stations in ODTS	36	60
Max. no. of stations in PPP	10	60
Max. data span in PPP	1 day	5 days
Max. data span in ODTS	2 days	5 days
Ftp upload	no	yes
Deletion of user station data	after 30 days	never
Usage of public station data	PPP only	PPP and ODTS
Share your station data	no	yes
Technical support by email	limited	next-day basis

<sup>(1)</sup> Orbits and clocks needed for PPP and COMP

<sup>(2)</sup> Needed for ODTS initialization

With *magicGNSS*, the user can analyze results in a convenient way through comprehensive PDF reports and organize the processing scenarios and history within his account in an easy way with a generous disk quota [9]. At present, *magicGNSS* supports GPS data, while GLONASS processing is planned for the end of 2009. One of the most interesting characteristics of *magicGNSS* is the easy way to use it. Inside the *magicGNSS* account, one has just to click on *New* to define a new scenario (network), then click on *Save*, and then click on *Run* to process the data and generate results.

The algorithms that process station data to generate solutions in *magicGNSS* are called ODTS, which stands for *Orbit Determination & Time Synchronization*, and PPP. ODTS is a *network solution* requiring a set of stations distributed worldwide. PPP is a *single-station solution* (although several stations can be processed together for convenience). In ODTS and PPP, the stations must be static. The advantages of a network solution compared to PPP are that the estimates of each station can benefit from the measurements of all stations. This should be, in principle, more robust and precise. In addition, all clock differences are available in a single solution instead of asking for a time-consuming series of PPP single-station solutions.

There are two types of station data within *magicGNSS*: *core station* data and *user station* data. For ODTS, the server maintains data from 36 IGS core stations distributed worldwide. Current *core station* data are available with a latency of typically 1 hour. The user (for \*pro\* account) can also upload his own station data (RINEX files) via the Web or ftp. Batch upload and automation are possible using ftp. Normal or compressed data files can be uploaded, and if the RINEX file does not have P1, the C1 code will automatically be converted to P1 using the CC2NONCC tool from IGS. Station data uploaded and shared by other users can also be processed.

The GPS operators inform the users about events affecting satellite availability by publishing messages named NANUs. *magicGNSS* automatically downloads NANUs as they are issued and extracts the relevant information so that only healthy satellites will be considered in the data processing. An additional module, called COMP, allows comparing *magicGNSS* products with IGS and among themselves. **Error! Reference source not found.** shows the products generated by *magicGNSS*.

Table 2. *magicGNSS* products.

Product	ODTS	PPP	Format	Accuracy (RMS)
Report	✓	✓	pdf	N/A
Satellite orbits	✓	✗	sp3	~2/6/4 cm <sup>(*)</sup>
Satellite clocks	✓	✗	clk	~0.10 ns
Station clocks	✓	✓	clk	~0.10 ns
Station tropo	✓	✓	txt	~5 mm (zenith)
Station coords	✓	✓	snx	<1 cm

(\*) In the Radial/Along/Normal directions

## DATA PROCESSING AND PRODUCTS

The basic ODTS and PPP input measurements are pseudorange (code) and phase L1-L2 dual-frequency iono-free combinations. On L1, the P1 code is used in order to be consistent with IGS. The raw input code and phase measurements are decimated and used internally by ODTS and PPP at a typical rate of 5 minutes (down to 30 sec can be used in PPP). The code measurements are smoothed using the phase with a Hatch filter, thus reducing the code error from the meter level to typically 25 cm.

ODTS and PPP are based on a batch least-squares algorithm that minimizes measurement residuals solving for orbits, satellite and station clock offsets, phase ambiguities, and station tropospheric zenith delays. In the case of PPP, satellite orbits and clocks are not solved for, but fixed to IGS products (*ultra-rapid*, *rapid*, or *final*). For this reason PPP is not a totally independent technique, unlike ODTS that, autonomously, provides all products.

Clocks are calculated as snapshot values, i.e., as instantaneous values at the measurement time epoch, without correlation to previous estimates. Clocks are estimated with a rate that typically is five minutes, conversely to the receivers measurements that are generated every second and, then, decimated to 30 seconds.

In ODTS, satellite and station clock offsets are estimated with respect to a reference clock provided by one of the stations and chosen by the user (taking into account that the overall clock stability could be affected by the stability of the chosen reference clock). In PPP, the station clock is referred to the IGS Time scale (IGST), as derived from the satellite clocks in the IGS products. From subsequent subtraction, the differences between station clocks can be inferred.

The satellite and Earth dynamics are based on high-fidelity models that follow IERS recommendations issued in 2003, trying to implement the partial updates that are published periodically, with some delay and only if they're relevant for *magicGNSS* application (it's not guaranteed that all updates have been considered). Modelled effects include a full Earth gravity model, Sun, Moon, and planetary attractions, solid Earth tides, ocean loading, and solar radiation pressure (SRP), including eclipses.

Radiation force discontinuities during eclipse entry/exit are smoothed in order to improve orbit accuracy. The satellite attitude is modelled as a generic nadir-pointing yaw-steering law applicable to all GNSS satellites. In ODTS, the orbit fit is based on the estimation of the initial state vector (position and velocity) and eight *empirical* SRP parameters. Earth Rotation Parameters (ERPs) are automatically downloaded from the IERS server, but they can also be estimated by ODTS itself. The tropospheric correction is based on the estimation of a zenith delay per station (a constant value every hour), using a mapping function to account for the satellite-station signal elevation. Small effects such as relativity and carrier-phase wind-up are also modelled.

For the core stations, *a priori* station coordinate values come from ITRF or IGS solutions, and they can be refined within the ODTS process. For user stations, the precise coordinates from PPP can be used as input values for ODTS. Satellite and station antenna offsets and phase center variations are taken into account; the latest ANTEX file from IGS is always used.

## DESCRIPTION OF THE ODTS ALGORITHM

The ODTS processing can be summarized as follows:

1. Given a satellite position and velocity at a certain starting epoch, an orbit can be produced on the basis of dynamic information, by numerical integration of the equations of motion of the satellite over a certain period. Furthermore, the partial derivatives of the satellite position with respect to the estimated dynamical parameters are produced.
2. For the epochs within that period at which tracking data are available, a tracking observation can be reconstructed numerically, using the known station position, the satellite position coming from the integrated orbit, and precise models for the effects affecting the tracking signal propagation. Also, the partial derivatives of the reconstructed measurements with respect to the estimated parameters are produced.
3. The measurement residuals (difference between the pre-processed tracking observations and the associated calculated observations) are computed.
4. The sum of the squares of all available residuals is minimized by estimating corrections to the various model parameters in a least-squares sense. To accomplish that, the computation of the partial derivatives of the expected measurements with respect to the estimated parameters is needed.

The process described is iterated until one of the following criteria is met:

- the number of iterations exceeds a certain threshold defined by configuration;
- the RMS of the weighted measurement residuals is below a certain threshold defined by configuration;
- the difference between two consecutive solutions is below a certain margin established by configuration.

The next sections describe those steps in detail.

## ORBIT COMPUTATION

The orbit propagation consists of computing the satellite state vector for a whole integration arc, given an initial state vector at the epoch  $t_0$  and a model of forces acting on the satellite. The solution of the problem is achieved by integrating the equations of motion, which can be expressed in matrix form as follows:

$$\begin{aligned}\frac{d\bar{y}}{dt} &= \bar{f}(t, \bar{y}) \\ \bar{y}(t_0) &= \bar{y}_0\end{aligned}$$

where

$$\begin{aligned}\bar{y} &= \begin{pmatrix} \bar{r} \\ \bar{v} \end{pmatrix}, & \bar{y}_0 &= \begin{pmatrix} \bar{r}_0 \\ \bar{v}_0 \end{pmatrix} \\ \bar{f}(t, \bar{y}) &= \begin{pmatrix} \bar{v} \\ \bar{a} \end{pmatrix}\end{aligned}$$

$\bar{r}$  and  $\bar{v}$  are the satellite position and velocity,  $\bar{a}$  is the acceleration, and  $\bar{y}_0$  is the state vector at the epoch  $t_0$ . The numerical integration of this differential equation is performed using an 8<sup>th</sup>-order Gauss-Jackson method. The state vector  $\bar{y}_0$  at the end of the estimation arc is one of the sets of parameters that have to be estimated during the ODTS process. After a preliminary integration using an approximate state vector (from navigation messages), the integration is always performed backwards, using the estimated state vector at the end of the arc as initial value.

The integration process is based on physical models, which provide the satellite acceleration at each moment in time, as a sum of all the contributions, namely earth and third body gravity, solar radiation pressure, and relativistic correction to acceleration.

## MEASUREMENT MODELLING

The main goal of this part of ODTS is to provide the least-squares module with the measurement residuals and partial derivatives of the measurements with respect to the parameters to be estimated.

This process has three parts, which have to be performed observation by observation:

- compute the measurement expected from the computed satellite orbit, the (possibly estimated) station positions, and an estimation of the different biases between the direct measurement and the geometric station-satellite distance: tropospheric delay, satellite and station clock biases, phase ambiguity, plus a relativistic correction
- compute the residual, that is, the difference between the actual measurement and the expected one
- get the partial derivatives of the expected measurement with respect to all the estimated parameters, using the partial derivatives of the orbit with respect to the dynamical parameters computed in the orbit integration.

The GNSS measurements accepted by ODTS can be of four different types:

- ❑ Raw iono-free pseudorange
- ❑ Smoothed iono-free pseudorange
- ❑ Iono-free carrier phase
- ❑ Ambiguity-free iono-free carrier phase.

The tropospheric delay can be configured to be removed either in pre-processing (which means they are “tropo-free”) or estimated within the ODTS process.

Note that the GNSS measurements have to be corrected to be referred to the center of mass of the satellite, and not to the satellite antenna phase center.

### EXPECTED MEASUREMENT COMPUTATION

All the computations are performed in the Inertial Reference Frame. To obtain the geometrical range  $d$  (in meters) for a measurement at reception time  $\tau$ , the following operations are necessary:

- compute actual reception time  $\tau - b_{sta}$ , where  $b_{sta}$  is the station clock bias
- compute station position at reception time:  $\bar{x}(\tau - b_{sta})$
- compute travel time:  $\Delta t = d_0/c + \Delta/c$ , where  $\Delta$  is the total correction to the travel time, in meters, due to different biases, and  $c$  the velocity of light
- satellite emission time is approximately

$$(\tau - b_{sta}) - \Delta t = (\tau - b_{sta}) - d_0/c - \Delta/c,$$

where  $d_0$  is an initial value for the geometric range, which is chosen to be  $\rho$  (the actual measurement), since the convergence is faster. Note that it would also converge to the solution taking  $d_0=0$  instead of  $d_0=\rho$ .

- compute satellite position at emission time:

$$\bar{r}(\tau - b_{sta} - d_0/c - \Delta/c)$$

- get geometrical range:

$$d_n = \|\bar{x}(\tau - b_{sta}) - \bar{r}(\tau - b_{sta} - d_0/c - \Delta/c)\|$$

This formula has to be iterated to obtain the correct value:

$$d_{n+1} = \|\bar{x}(\tau - b_{sta}) - \bar{r}(\tau - b_{sta} - d_n/c - \Delta/c)\|$$

Finally, the expected measurement (in meters) is just the final travel time (in meters), corrected by the effect of the clock biases:

$$\rho_{exp} = d + \Delta + \delta t_{rel} + b_{sta} - b_{sat}$$

where  $b_{sat}$  is the satellite clock bias, and  $\delta t_{rel}$  is the relativistic correction to the satellite clock.

When the measurement is carrier-phase, the formula is slightly different:

$$\varphi_{\text{exp}} = d + \Delta + \delta t_{\text{rel}} + b_{\text{sta}} - b_{\text{sat}} - \text{Amb}$$

where  $\text{Amb}$  is the estimated ambiguity (pass-dependent bias).

The corrections included in the term  $\Delta = D_{\text{Tropo}} + c \cdot \Delta t_r$  are:

- $D_{\text{Tropo}}$  - tropospheric delay, either computed in pre-processing or to be estimated in ODTS
- $\Delta t_r$  - relativistic correction to the travel time.

Note that  $\delta t_{\text{rel}}$  and  $\Delta t_r$  are different terms: the first one is a correction to the satellite clock, and  $\Delta t_r$  is the correction to the travel time.

## STATION AND SATELLITE POSITION COMPUTATION

For the process described above, we should be able to get the satellite and station position at any time. In the case of the satellite, we just use the orbit obtained by the orbit integrator at fixed steps, and interpolate at required time using a Lagrange of 8<sup>th</sup> order.

The station positions passed to ODTS are in ECEF coordinates. These are not the geodetic marker coordinates, but the antenna phase center. In order to get the station position in the inertial frame, the Earth Rotation Matrix is also interpolated by Lagrange at required time:  $[\text{ERM}(t)]$ . The station position in IRF (Inertial Reference Frame) results from applying the Earth Rotation Matrix to the estimated station position in ECEF:

$$\vec{x}_{\text{STA\_IRF}} = [\text{ERM}(t)] \vec{x}_{\text{STA\_ECEF}}$$

The station position is subject to periodic variations due to solid tides, ocean loading, and atmospheric loading. ODTS only retains the first contribution, the instantaneous deformation of the solid Earth under the tidal potential of the Sun and the Moon. The vector displacement of the station due to degree 2 Solid Earth Tides expressed in the inertial reference frame is given by:

$$\Delta \vec{x}_j = \sum_{k=1}^2 \frac{GM_k a_e^4}{GM_{\oplus} \|\vec{x}_{P,k}\|^3} \left\{ h_2 \vec{x}_j \left( \frac{3}{2} (\vec{x}_{P,k} \cdot \vec{x}_j)^2 - \frac{1}{2} \right) + 3l_2 (\vec{x}_{P,k} \cdot \vec{x}_j) \left[ \vec{x}_{P,k} - (\vec{x}_{P,k} \cdot \vec{x}_j) \vec{x}_j \right] \right\}$$

where:

$GM_1$	Gravitational constant of the Sun
$GM_2$	Gravitational constant of the Moon
$a_e$	Equatorial radius of the Earth
$\vec{x}_{P,1} = \vec{x}_{\text{Sun}}$	Inertial position of the Sun
$\vec{x}_{P,2} = \vec{x}_{\text{Moon}}$	Inertial position of the Moon
$h_2$	Degree 2 Love number (= 0.6026)
$l_2$	Degree 2 Shida number (= 0.0831).

This formula comes from the IERS 1996 conventions, and corresponds to the elastic Earth approximation.

## CLOCK BIASES

A satellite or station clock is supposed to be a realization of its local time, but in fact it has a bias with respect to the true time  $t$  (which a perfect clock would provide):

$$\tau = t + b$$

where  $\tau$  is the clock reading and  $b$  is the clock bias.

The clock bias is estimated by the least-squares process for each observation epoch. The relativistic effect on the satellite clocks has been also considered, whose most important part is the eccentricity correction:

$$\delta t_{rel} = + \frac{2\vec{r} \cdot \vec{v}}{c^2}.$$

## CORRECTIONS TO TRAVEL TIME

In the previous description of the measurement reconstruction, the term  $\Delta$  consists of the several corrections to the travel time, namely:

### Tropospheric Delay:

The tropospheric delay can be either computed by the pre-processing algorithm or estimated in ODTS.

In the first case, the delay is just taken from the observations input structure.

In the second case, the tropospheric zenith delay is the parameter to be estimated during the ODTS process. The tropospheric delay for a given elevation angle is obtained from the zenith delay by a mapping function, chosen by configuration between the Saastamoinen model and an external model.

The Saastamoinen model has the following mapping function:

$$D = \frac{D_z - 0.002277 * B * (\cot E)^2}{\sin E}$$

where  $E$  is the elevation angle and  $D_z$  is the zenith delay. The correction term  $B$  depends on the station altitude, and can be interpolated from a table.

### Relativistic Correction:

This is the correction due to general relativity theory, whose most important effect is the Shapiro delay [10]. Note that the ionospheric delay is not computed, since the ODTS input observable is iono-free.

## RESIDUALS COMPUTATION

The residuals are the difference between the expected measurements  $\rho_{exp}$  and the actual measurements  $\rho$  obtained at the receivers. If there were no measurement noise, and if our orbits, clocks, and corrections were the exact ones, the residuals should be zero. If our estimation of orbits, clocks, and our corrections are accurate, the residuals contain essentially the measurement noise. The residuals computation is simply, for any measurement type:

$$res = \rho - \rho_{exp}$$

$$res = \varphi + ambiguity - \varphi_{exp}$$



## TIME AND FREQUENCY TRANSFER EVALUATION SCENARIO

A preliminary evaluation of the time transfer capabilities of *magicGNSS* has been carried out selecting a network of eight GNSS stations belonging to six laboratories contributing to TAI and considered in the BIPM TAI PPP experiment, as indicated in **Error! Reference source not found.**

Table 3. Timing labs and GPS receivers involved in the experiment.

Laboratory	TAI code	Country	Station name	Receiver type	Reference
INRIM	IE	Italy	ieng	Ashtech Z-XII3T	UTC(IT)
ORB	OR	Belgium	brus	Ashtech Z-XII3T	UTC(ORB)
PTB	PT	Germany	ptbb	Ashtech Z-XII3T	UTC(PTB)
ROA	RO	Spain	roap	Septentrio PolaRx-3TR	UTC(ROA)
SP	SP	Sweden	sp01	Javad JPS GGD	UTC(SP)
SP	SP	Sweden	sp02	Javad JPS GGD	UTC(SP)
SP	SP	Sweden	spt0	Javad JPS GGD	External H-Maser
USNO	US	United States	usn3	Ashtech Z-XII3T	UTC(USNO)

A total of 39 GPS stations are used in the ODTS algorithm, i.e. the eight *user stations* and 31 *core stations* from IGS. The experiment duration was between 31 Oct and 19 Nov 2009 (DOY 304-323; MJD 55135-55154).

Hourly RINEX files, generated by considered receivers and uploaded onto a dedicated *magicGNSS* account, have been processed by means of the ODTS algorithm with respect to the IENG station clock, chosen as reference. Batches of 2-day duration have been processed in ODTS. This is a compromise between data processing computer speed and clock solution continuity.

The RINEX data are uploaded and processed in near-real time using the Scheduler in *magicGNSS*. The Scheduler runs every hour at 20 minutes after the hour. This delay is on purpose to account for the station data latency and upload time. The ODTS process takes around 5 minutes to complete; therefore, synchronization results are typically ready 30 minutes after the hour, for the last hour and before.

A comparison with the estimates generated by *magicGNSS*, PPP, and NRCAN PPP algorithms, together with IGS (*rapid* products), has been performed in terms of phase offsets and frequency stability.

## RESULTS

In the next figures, the USN3-IENG baseline estimates are reported as an example, as generated by both *magicGNSS* ODTS and PPP algorithms, together with IGS (*rapid* products) outputs.

For the purpose of plotting, for each of the time series its own mean value and linear drift have been removed. Evaluations of the Allan deviations are also reported.

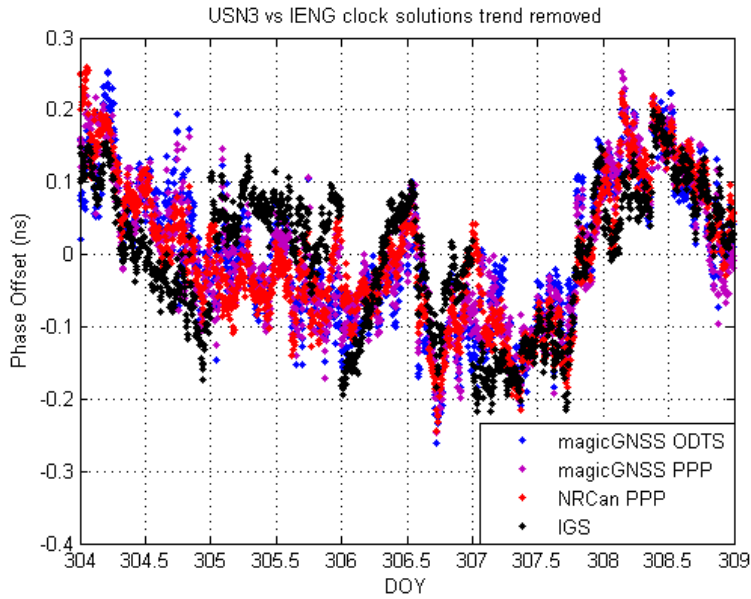


Figure 1. USN3-IENG baseline clock estimates as obtained with *magicGNSS* ODTs and PPP algorithms, together with IGS (rapid products).

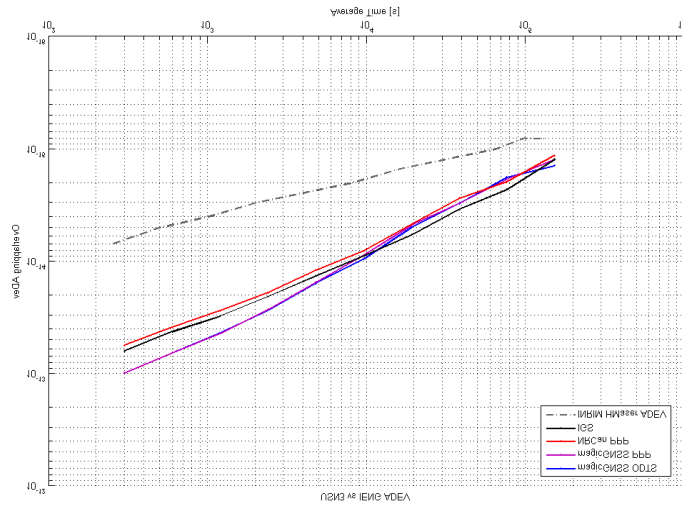


Figure 2. USN3-IENG baseline clock estimates frequency stability, as obtained with *magicGNSS* ODTs and PPP algorithms, together with IGS (rapid products).

The two time scales comparison results and the frequency stability analysis show a good overall agreement among the estimates generated by the different synchronization techniques (two H-Masers in the case of INRIM and USNO). In particular, it seems that the ODTs technique, even in case of a limited network of 39 stations, offers clock comparisons with a precision that is comparable to the state-of-the-art techniques, such as PPP or IGS products.

A higher short-term noise is observed in the ODTs and PPP solutions from *magicGNSS*. This is believed to be due to the *snapshot* clock estimation in *magicGNSS* (the clocks are estimated as independent values at each epoch, without any constraint with previous clock values), as opposed to sequential filter solutions (NRCAN PPP) or clock averages from different Analysis Centers (IGS), which tend to smooth the short-term clock estimation error.

For completeness, Figure 3 shows the clock stability of all timing stations with respect to IENG, from ODTs results.

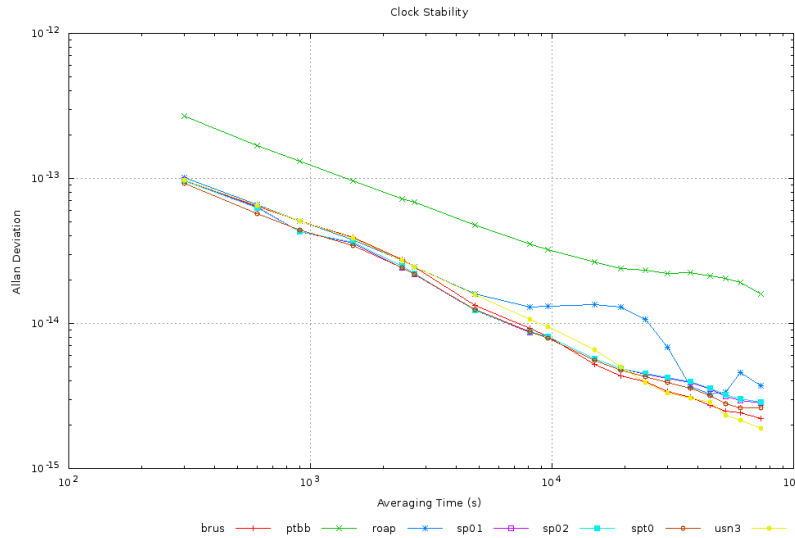


Figure 3. Clock stability vs. IENG from ODTs.

Another complementary assessment can be obtained by comparing the clock difference between GPS *satellite* clocks as provided by *magicGNSS* ODTs and the same ones provided by the IGS (this kind of evaluation is provided automatically by *magicGNSS* ODTs), considered as reference. IGS solutions take advantage of the highest number of stations tracking GPS in the IGS network (>350); the different software and strategies used by different IGS Analysis Centers, a stable reference frame, and most important clock solutions are computed against IGS time scale, avoiding any instability introduced by the reference station used by the ODTs. For the considered network, the total RMS difference is around 0.12 ns (see Figure 4) and this quantity can be used as an indirect indicator of the precision of the station clocks estimates. Improvements can be achieved adding more network stations and distributing the network in a more global way.

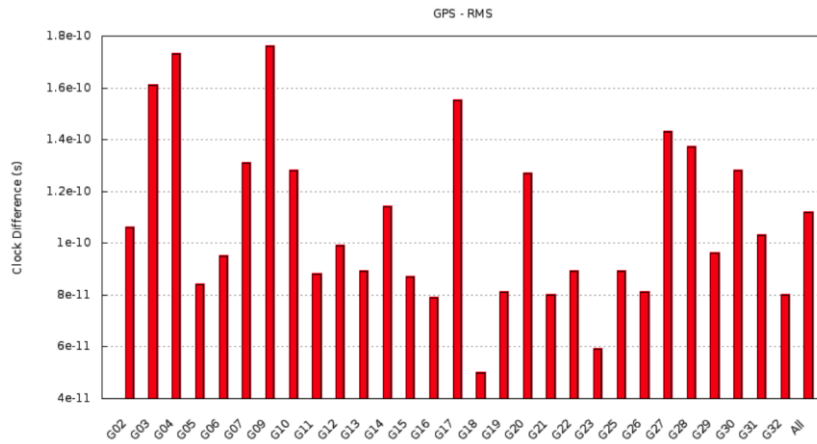


Figure 4. ODTs vs. IGS clock comparison for the GPS satellites.

An additional experiment has been carried out to assess the applicability of the ODTS technique to small station networks. In particular, what accuracy can we obtain if we process only the eight timing stations in ODTS. The results show that, even if globally, the orbit determination and clock synchronization is greatly degraded, for short baselines satellite orbit and clock errors largely cancel out, and for continental links the clock synchronization accuracy is nearly as good as when using a global network, but not so for intercontinental links.

This is shown in Figure 5, to be compared with Figure 3. Notice that, except for the intercontinental USN3-IENG link (America-Europe, yellow line), the rest of the European baselines do not show much degradation with respect to the global ODTS network.

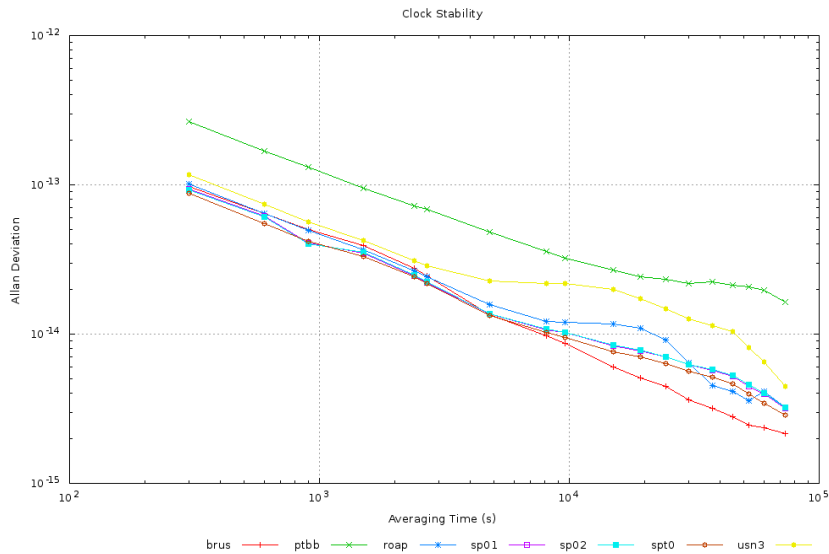


Figure 5. Clock stability vs. IENG from ODTS, using only eight stations.

In order to assess the presence of the so-called “batch boundary discontinuities” in *magicGNSS* outputs (both ODTS and PPP algorithms), for the USN3-IENG baseline, three consecutive 5-day-batch processing has been performed and compared with the same estimates gotten by using the PPP algorithm developed by NRCan and IGS estimates that are estimated on daily batches. Results are reported in Figures 6 and 7.

The accuracy of GPS-based time and frequency transfer using combined analysis of code and carrier-phase measurements greatly depends on the noise of the GPS signals. In particular, the pseudorange noise is responsible for batch-boundary discontinuities that can reach, for some stations, more than 1 ns in the time transfer results obtained from geodetic analysis. These discontinuities are caused by the fact that the data are analyzed in batches and, within each batch, the station clock offset and carrier-phase ambiguities are estimated by the observed pseudoranges.

The pseudorange noise is sometimes and for some stations not white noise, for example, because of near-field multipath effects or variation of instrumental delays. The averaging of this colored pseudorange noise induces clock datum changes between (daily) batches at the level of a few hundred ps to a few ns [11]. IGS uses daily batches; therefore, the boundary jumps are visible from day to day. PPP is based on the IGS estimates and, therefore, may inherit this effect. *magicGNSS* at the moment is used on batches of 5 days and, therefore, the boundary jumps are mostly visible on those boundaries. The effect of batch boundary jumps can be reduced through averaging over multi-day intervals of different duration [4] or mixing GPS geodetic results with other independent techniques, such as the TWSTFT.

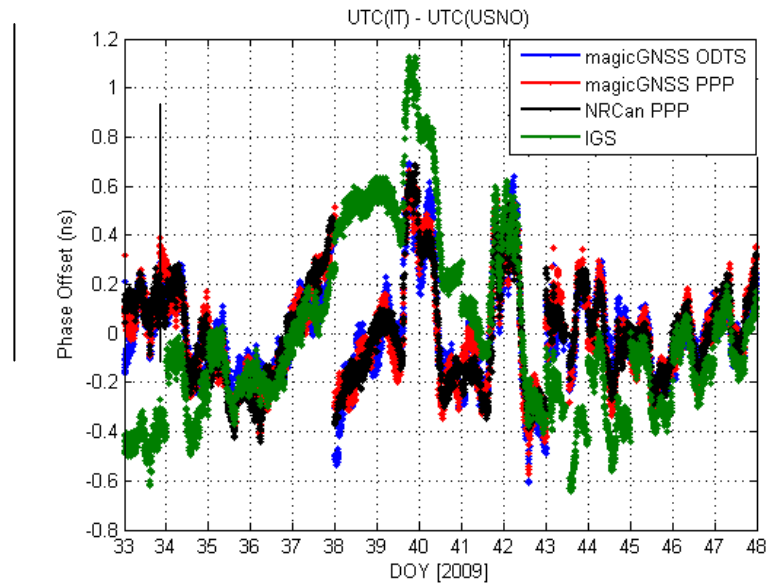


Figure 6. USN3-IENG baseline clock estimates as obtained with *magicGNSS* ODTs and PPP algorithms, together with NRCAN PPP and IGS (rapid products) outputs.

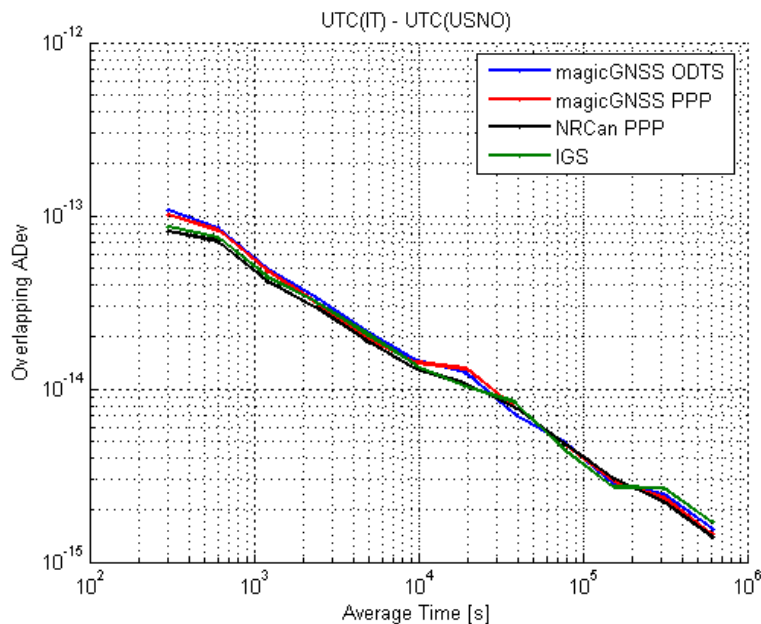


Figure 7. USN3-IENG baseline clock estimates' frequency stability, as obtained with *magicGNSS* ODTs and PPP algorithms, together with NRCAN PPP and IGS (rapid products) outputs.

## CONCLUSIONS

The presented work represents a preliminary investigation about the time/frequency transfer capabilities of the *magicGNSS* web application, in near-real time with a typical latency of 30 minutes in the results. First outcomes show promising performances.

The results presented in this paper can be browsed in near-real time on the following *live* Web page: <http://magicgnss.gmv.com/ptti>.

More investigations are in progress taking into account different periods and different types of networks, looking also at the robustness and reliability of the algorithm. Also, since that, through PPP/ODTS techniques the clocks are “seen” at the receiver phase center antenna (measures are not “calibrated”), in future work “calibration” issues will be specifically addressed.

## ACKNOWLEDGMENTS

Authors wish to thank all the people in timing laboratories involved in this experiment for granting the use of their GPS data; the Geodetic Survey Division, Natural Resources Canada (NRCan), for providing the NRCan PPP software; and the International GNSS Service (IGS) for providing good quality data and products.

## REFERENCES

- [1] J. Levine, 2008, “*A review of time and frequency transfer methods*,” **Metrologia**, **45**, S162-S174.
- [2] P. Defraigne, G. Petit, and C. Bruyninx, 2002, “*Use of geodetic Receivers for TAI*,” in Proceedings of the 33rd Annual Precise Time and Time Interval (PTTI) Systems and Applications Meeting, 27-29 November 2001, Long Beach, California, USA (U.S. Naval Observatory, Washington, D.C.), pp. 341-348.
- [3] D. Orgiazzi, P. Tavella, and F. Lahaye, “*Experimental assessment of the Time Transfer Capability of Precise Point Positioning (PPP)*,” in Proceedings of the 2005 Joint IEEE International Frequency Control Symposium (FCS) and Precise Time and Time Interval (PTTI) Systems and Applications Meeting, 29-31 August 2005, Vancouver, British Columbia, Canada (IEEE 05CH37664C), pp. 337-345.
- [4] N. Guyennon, G. Cerretto, P. Tavella, and F. Lahaye, 2009, “*Further Characterization of the Time Transfer Capabilities of Precise Point Positioning (PPP)*,” **IEEE Transactions on Ultrasonics, Ferroelectrics, and Frequency Control**, **UFFC-56**, 1634-1641.
- [5] P. Defraigne, C. Bruyninx, and N. Guyennon, 2007, “*PPP and phase only GPS frequency transfer*,” in Proceedings of the IEEE International Frequency Control Symposium (FCS) Jointly with the 21<sup>st</sup> European Frequency and Time Forum (EFTF), 29 May-1 June 2007, Geneva, Switzerland, pp. 904-908.
- [6] P. Defraigne, Q. Baire, and N. Guyennon, 2007, “*GLONASS and GPS PPP for time and frequency transfer*,” in Proceedings of the IEEE International Frequency Control Symposium (FCS) Jointly with the 21<sup>st</sup> European Frequency and Time Forum (EFTF), 29 May-1 June 2007, Geneva, Switzerland, pp. 909-913.
- [7] G. Petit and Z. Jiang, 2008, “*Precise Point Positioning for TAI computation*,” **International Journal of Navigation and Observation**, **2008**, Article ID 562878.
- [8] J. Kouba and P. Héroux, 2001, “*Precise Point Positioning Using IGS Orbit and Clock Products*,” **GPS Solutions**, **5**, No. 2, 12-28.
- [9] R. Piriz, A. Mozo, P. Navarro, and D. Rodriguez, 2008, “*magicGNSS: Precise GNSS Products Out of the Box*,” in Proceedings of the 21<sup>st</sup> International Technical Meeting (ION GNSS), 16-19 September 2008, Savannah, Georgia, USA (Institute of Navigation, Alexandria, Virginia), pp. 1242-1251.
- [10] B. W. Parkinson and J. J. Spilker (editors), 1996, **Global Positioning System: Theory and Applications**, **Vol. I** (American Institute of Aeronautics, Washington, D.C.), p. 690.

- [11] P. Defraigne and C. Bruyninx, 2007, “*On the link between GPS pseudorange noise and day boundary discontinuities in geodetic time transfer solutions,*” **GPS Solutions**, **11**, No. 4, 239-249.

